Journal of the American Heart Association

ORIGINAL RESEARCH

Distinct Exercise Response Patterns in Patients With Heart Failure With Preserved Ejection Fraction

Stephanie De Schutter, MD; Nicola R. Pugliese, MD, PhD; Laura M. G. Meems, MD, PhD; Sara Moura-Ferreira, MD; Nicolò De Biase, MD; Lavinia Del Punta, MD; Stefano Masi, MD, PhD; Jan Stassen, MD, PhD; Lieven Herbots, MD, PhD; Guido Claessen, MD, PhD; Caroline M. Van de Heyning, MD, PhD; Jan Verwerft, MD, PhD; Andreas B. Gevaert, MD, PhD

BACKGROUND: Heart failure with preserved ejection fraction (HFpEF) is a heterogeneous disease characterized by exercise intolerance. Defining pathophysiologically distinct subgroups allows more personalized therapy, but efforts mainly relied on resting examinations. This study aimed to define HFpEF phenotypes based on exercise limitations using combined cardiopulmonary exercise testing with stress echocardiography.

METHODS: A total of 913 patients with HFpEF were recruited from 4 third-line centers and divided into derivation (n=623) and validation cohorts (n=290). Unsupervised graph-based clustering of 61 cardiopulmonary exercise testing with stress echocardiography variables was used to identify HFpEF exercise phenotypes. Pathophysiological characteristics, exercise capacity, and clinical outcomes were compared between phenotypes.

RESULTS: In the derivation cohort, cluster analysis identified 5 distinct HFpEF exercise phenotypes characterized by specific exercise responses: mild diastolic dysfunction (phenotype 1), impaired peripheral oxygen extraction (phenotype 2), right ventricular-pulmonary artery uncoupling (phenotype 3), reduced left ventricular systolic reserve (phenotype 4), and chronotropic incompetence (phenotype 5). The composite outcome of all-cause death and unplanned cardiovascular hospitalization differed significantly across phenotypes, with phenotypes 2 (hazard ratio [HR], 1.76 [95% CI, 1.07–2.91]), 4 (HR, 2.15 [95% CI, 1.27–3.65]), and 5 (HR, 2.19 [95% CI, 1.33–3.61]) showing higher rates of the primary combined outcome compared with phenotype 1. All phenotypes were replicated in the validation cohort.

CONCLUSIONS: Deep phenotyping of the exercise response in patients with HFpEF revealed 5 distinct phenogroups with marked differences in pathophysiology, exercise performance, and clinical outcomes. This subclassification may support more personalized therapeutic strategies and improve risk stratification in HFpEF.

Key Words: cardiopulmonary exercise test ■ exercise echocardiography ■ exercise physiology ■ HFpEF ■ phenotype

Heart failure (HF) with preserved ejection fraction (HFpEF) is the most prevalent type of HF, and its prevalence is expected to further increase due to population aging.[1] Compared with HF with reduced EF, the prognosis of HFpEF is equally poor and current pharmacological options for improving HFpEF prognosis remain limited.[2] Established therapies include sodium-glucose cotransporter 2 inhibitors (SGLT2i), mineralocorticoid antagonists, and rigorous management of comorbidities.[3] However, the burden of hospitalizations and mortality remains significant.[4] A potential explanation is the heterogeneity of HFpEF.

Correspondence to: Stephanie De Schutter, MD, University of Antwerp, Research group Cardiovascular Diseases, GENCOR Department, Universiteitsplein 1, 2610 Antwerp, Belgium. Email: stephanie.deschutter@uantwerpen.be

This article was sent to Yen-Hung Lin, MD, PhD, Associate Editor, for review by expert referees, editorial decision, and final disposition.

Supplemental Material is available at https://www.ahajournals.org/doi/suppl/10.1161/JAHA.126.050524

For Sources of Funding and Disclosures, see page 1.

JAHA is available at: www.ahajournals.org/journal/jaha

CLINICAL PERSPECTIVE

What Is New?

- Exercise-based clustering of combined cardiopulmonary exercise testing with stress echocardiography data identified 5 heart failure with preserved ejection fraction phenotypes with different exercise responses including mild diastolic dysfunction, impaired peripheral oxygen extraction, right ventricular-pulmonary artery uncoupling, reduced left ventricular systolic reserve, and chronotropic incompetence.
- The heart failure with preserved ejection fraction exercise phenotypes showed marked differences in exercise capacity and clinical outcomes.

What Are the Clinical Implications?

- This subclassification is a step towards personalized, targeted treatment strategies and may improve risk stratification in heart failure with preserved ejection fraction.

Nonstandard Abbreviations and Acronyms

CPET	cardiopulmonary exercise testing
CPETecho	combined cardiopulmonary exercise testing and stress echocardiography
HFA-PEFF	Heart Failure Association Pretest probability, Echocardiography and natriuretic peptide score, Functional testing, and Final aetiology algorithm
H_2FPEF	Heavy, Hypertensive, Atrial Fibrillation, Pulmonary Hypertension, Elder, Filling Pressure Score
HFpEF	heart failure with preserved ejection fraction
PAP	pulmonary artery pressure
PC	principal component
SGLT2i	Sodium-glucose cotransporter 2 inhibitors
VO_2	oxygen consumption

Several clinical trials that failed to improve the primary outcome later identified subgroups of patients with HFpEF who responded favorably to the tested treatment.[5] Identifying these subgroups has sparked the hypothesis that patients with HFpEF can be classified according to mutually exclusive "phenotypes," which share clinical and pathophysiological characteristics. Identifying these HFpEF phenotypes may identify specific subgroups with HFpEF more amenable to therapy, supporting more personalized and effective treatment. Several research groups have classified patients into phenotypes based on clinical characteristics, biomarkers, and imaging profiles.[6–10] As exercise intolerance is the hallmark symptom of HFpEF, we hypothesize that a subclassification based on the response to exercise may be specifically relevant for therapeutic decisions and clinical outcomes.

Combined cardiopulmonary exercise testing and stress echocardiography (CPETecho) is a relatively new modality which can characterize the entire pathway of O_2 transport and utilization noninvasively, fully characterizing limits to exercise capacity.[11,12] CPETecho is used in specialized centers to identify patients with HFpEF at an early stage, as resting hemodynamics and echocardiography are normal in up to one third of patients with HFpEF.[11,13] Exercise may provoke increased left ventricular (LV) filling pressures in up to 64% of patients with unexplained dyspnea and normal resting examinations.[5,14] In this study, we aimed to better characterize the heterogeneity of exercise physiology in patients with HFpEF by classifying those with confirmed HFpEF into different phenotypes based on their exercise limitations using CPETecho.

METHODS

The data underlying this article will be shared at a reasonable request by the corresponding author. The study complied with the Declaration of Helsinki and was approved by the medical ethics committees of all participating centers (Ethisch Comité UZA/UAntwerpen: 002732, Medisch-Ethische Toetsingscommissie UMCG: 202100279, Ethisch Comité Jessa Ziekenhuis: 2020/014, University Hospital Pisa Bioethical Committee: 19204). Participants provided written informed consent.

Study Population

We retrospectively analyzed patients with HFpEF who underwent CPETecho between August 2016 and September 2023 in 4 third-line hospitals: Antwerp University Hospital (Edegem, Belgium), Jessa Hospital Hasselt (Hasselt, Belgium), University Medical Centre Groningen (Groningen, the Netherlands), and University Hospital Pisa (Pisa, Italy). All patients who underwent CPETecho were initially screened. Exclusion criteria were a left ventricular ejection fraction <50%, other structural heart disease (restrictive or hypertrophic cardiomyopathy, congenital heart disease), >moderate valvular stenosis or regurgitation, suspected coronary ischemia or age under 18 years. Among these, patients

meeting diagnostic criteria for HFpEF according to the 2021 European Society of Cardiology guidelines were selected: (1) symptoms and signs of HFpEF, (2) left ventricular ejection fraction ≥50%, and (3) objective evidence of cardiac structural or functional abnormalities consistent with the presence of LV diastolic dysfunction or raised LV filling pressures.[15] Patients recruited in Antwerp, Hasselt, and Groningen were designated as the derivation cohort, and patients recruited in Pisa served as the validation cohort. This division was based on geographic differences to enhance the generalizability of the findings.

CPETecho Procedure

CPETecho was performed as described previously, by experienced cardiologists (A.B.G., J.V., L.M.G.M., and N.R.P.).[11,12,16] All centers followed the same standardized protocol. Table S1 provides an overview of the equipment used per center. Patients performed a symptom-limited maximal exercise bout on a semisupine bicycle ergometer with a gradual workload increase (5–20 Watts/min), tailored to each patient's age, sex, weight, and functional status. An exercise duration of 8 to 12 minutes was targeted to reach peak oxygen consumption (VO_2). The protocol included 2 minutes of unloaded pedaling before exercise, and 3 minutes of recovery after peak effort. At rest, submaximal exercise, and peak exercise, echocardiography was performed. The submaximal stage corresponded to a heart rate of ~100 beats per minute, allowing Doppler measurements before E- and A-wave fusion occurs.[17] For peak imaging, acquisition was initiated once the respiratory exchange ratio exceeded 1.00 allowing sufficient time to complete the full imaging sequence, or at the point of symptom-limited exhaustion. If needed, a brief constant-load phase was added to allow completion of imaging, ensuring that key hemodynamic measurements could be obtained at respiratory exchange ratio ≥1.05. At each stage, the following parameters were sequentially collected: LV volumes (end-diastolic and end-systolic), left ventricular ejection fraction, E-wave, and A-wave velocities, e' at the septal and lateral mitral annulus, s' at the septal mitral annulus, s' at the lateral tricuspid annulus, tricuspid annular plane systolic excursion, stroke volume, and tricuspid regurgitation velocity to estimate pulmonary artery pressure (PAP). To improve PAP measurement accuracy, 1 to 3 mL of agitated colloid was routinely injected intravenously at each stage. The presence of B-lines was assessed by scanning 4 chest zones (third and fourth intercostal spaces at the mid and anterior axillary line on each side) at rest and immediately after maximal exercise.[18] Combining exercise echocardiography with CPET adds measurement of breath-by-breath minute ventilation, carbon dioxide production, and VO_2, enabling calculation of peripheral oxygen extraction. Respiratory gases, heart rate, 12-lead ECG, and noninvasive arterial saturation were recorded continuously. Additionally, spirometry was performed at rest to calculate breathing reserve (40×forced expiratory volume in 1 second), and laboratory tests including NT-proBNP (N-terminal pro B-type natriuretic peptide) measurement (Roche) were measured locally before the exercise test. VO_2peak was defined as the highest 30-second average VO_2 within the last minute of exercise. Predicted VO_2peak was calculated according to the Wasserman–Hansen equation for all participating centers.[19] CPETecho thus provided a comprehensive, noninvasive assessment of cardiac function, hemodynamics, and respiratory-metabolic parameters.

Clustering Analysis

Statistical analysis was performed using R version 4.4.1 (R Foundation for Statistical Computing, Vienna, Austria). Table S2 outlines the continuous variables obtained from CPETecho used as phenotypic features, encompassing echocardiographic, CPET, and spirometry data, along with heart rate, blood pressure, and arterial saturation measured both at rest and during exercise. Variables with <40% missing data were imputed using the Midastouch method, a predictive mean matching–based approach that preserves the observed data distribution and is robust to nonnormality. Those with >40% missing data were excluded from the analysis. To assess the impact of imputation, we performed Kolmogorov–Smirnov testing to compare pre- and postimputation distributions (Table S2; Data S1); for variables with significant differences, an additional tipping point analysis was conducted by perturbing imputed values (±1 SD) and evaluating cluster stability using the Adjusted Rand Index (Figure S1; Data S1). Before analysis, CPETecho variables were normalized using log transformation and scaled by *Z*-score standardization. Sixty-one continuous variables were input for graph-based clustering using the Shared Nearest Neighbor technique with the Louvain algorithm (Seurat package version 5.1.0), selected for its effectiveness in detecting meaningful clusters in complex, high-dimensional data by focusing on shared local relationships. Before clustering, dimensionality reduction was performed through principal component analysis, while uniform manifold approximation and projection was also used for visualization to simplify high-dimensional data into 2 or 3 dimensions. The clustering resolution (an essential parameter directly related to the number of clusters) was determined using a majority vote principle across three complementary, a priori defined methods: clustering trees, gap statistic and NbClust (Figure S2, Data S1).[20–22] The optimal resolution maximizes both within-cluster

similarity and between-cluster differences. As sensitivity analyses, clustering was repeated using the Leiden algorithm as an alternative community detection method, and the analysis was restricted to patients with an Heavy, Hypertensive, Atrial Fibrillation, Pulmonary Hypertension, Elder, Filling Pressure Score (H_2FPEF) score ≥6, testing the robustness of the clustering across different HFpEF definitions. For validation of the transferability of these phenotypes to an external population, mutual nearest neighbors were identified between the derivation and validation cohort, as described by Stuart et al., enabling comparison of phenotypes across different cohorts.[23] Additionally, we quantified the consistency in variable expression between phenotypes across derivation and validation cohorts using intraclass correlation coefficients and Bland–Altman analysis to detect potential systematic shifts.

Outcome Assessment

All study participants were followed for at least 6 months after CPETecho. The primary outcome was the time to the first occurrence of a composite end point, defined as all-cause death or unplanned cardiovascular hospitalization. This outcome was determined through a retrospective chart review, additionally querying a nationwide database for Belgian centers and telephone contact with patients for Pisa and Groningen.

Statistical Analysis

Continuous variables were presented as mean±SD and compared using ANOVA, after confirming normality of residuals and homogeneity of variance using the Brown–Forsythe test. When variances were unequal but data were normally distributed, Welch's ANOVA was applied. If nonnormally distributed, variables were presented as median (25th percentile–75th percentile) and compared using the Kruskal–Wallis test. Categorical variables were presented as n (%) and compared between groups using chi-square test. When overall group differences were significant, post hoc pairwise comparisons were performed. For the outcomes analysis, we employed both unadjusted and multivariable-adjusted Cox proportional hazards models to assess the independent association between phenotype groups and clinical outcomes (Survival package version 3.8.3). Covariates included in the adjusted models were selected a priori based on established prognostic relevance in HFpEF, and included age, sex, body mass index, estimated glomerular filtration rate, hemoglobin, NT-proBNP, and HFpEF risk scores. Proportional hazards assumption was assessed using Schoenfeld residuals. Kaplan–Meier curves stratified by phenotype were generated, with differences between groups tested using the log-rank test. *P* value <0.05 was considered significant.

RESULTS

Population Characteristics

Of 2306 patients screened, a total of 913 patients with HFpEF were included: 623 in the derivation cohort and 290 in the validation cohort (Figure 1). Baseline characteristics of the study population are displayed in Table 1. Overall, patients were predominantly female (56%), with a mean age of 74±8 years. The most prevalent comorbidities included hypertension (73%), atrial fibrillation (41%), diabetes (20%), and coronary artery disease (19%). Patients with HFpEF in the validation cohort were slightly older, more often men, and had similar prevalences of comorbidities, higher NT-proBNP, and more severe diastolic dysfunction and cardiac remodeling (Table 1).

Clustering Optimization

We used multiple approaches to define the optimal resolution for clustering, that is, the number of subgroups (Figure S2). Both clustering trees and NbClust identified 5 clusters as optimal, whereas the gap statistic suggested 4 clusters. As 2 of the 3 methods supported a 5-subgroup model, we proceeded with 5 clusters in further analyses.

After dimensionality reduction, we identified 9 principal components (PCs), capturing key differences between clusters. The main results were as follows: PC1 was primarily driven by cardiac index (factor loading [FL] 0.30), with the mean PAP/cardiac output slope contributing negatively (FL −0.24). PC2 was mainly influenced by variables related to peripheral oxygen extraction (FL 0.29) and negatively by indexed stroke volume (FL −0.26). Heart rate response was the dominant factor in both PC3 (FL 0.26) and PC5 (FL 0.27), whereas PC4 was positively associated with aerobic capacity (FL 0.32) and negatively with ventilatory efficiency (FL −0.27). Additional details on PCs and their contributing variables are provided in Figure S3. Differences between clusters are visualized in 2-dimensional and 3-dimensional plots of uniform manifold approximation and projection embeddings (Figure 2, Video S1). To assess the impact of imputation, we performed Kolmogorov–Smirnov tests and a tipping point analysis. Only 8 of 61 variables had a significantly different distribution after imputation; perturbing these variables ±1SD revealed stable clustering (Adjusted Rand Index ≥0.62) (Table S2, Figure S1).

Description of CPETecho-Based Clusters

Each of the 5 clusters exhibited marked differences in exercise pathophysiology (Table 2; Figure 3). Phenotype 1 (n=93, 15% of the derivation cohort) exhibited only mild diastolic dysfunction with preserved biventricular systolic reserve. Patients with phenotype 2 (n=131, 21%) had lower peripheral oxygen extraction difference

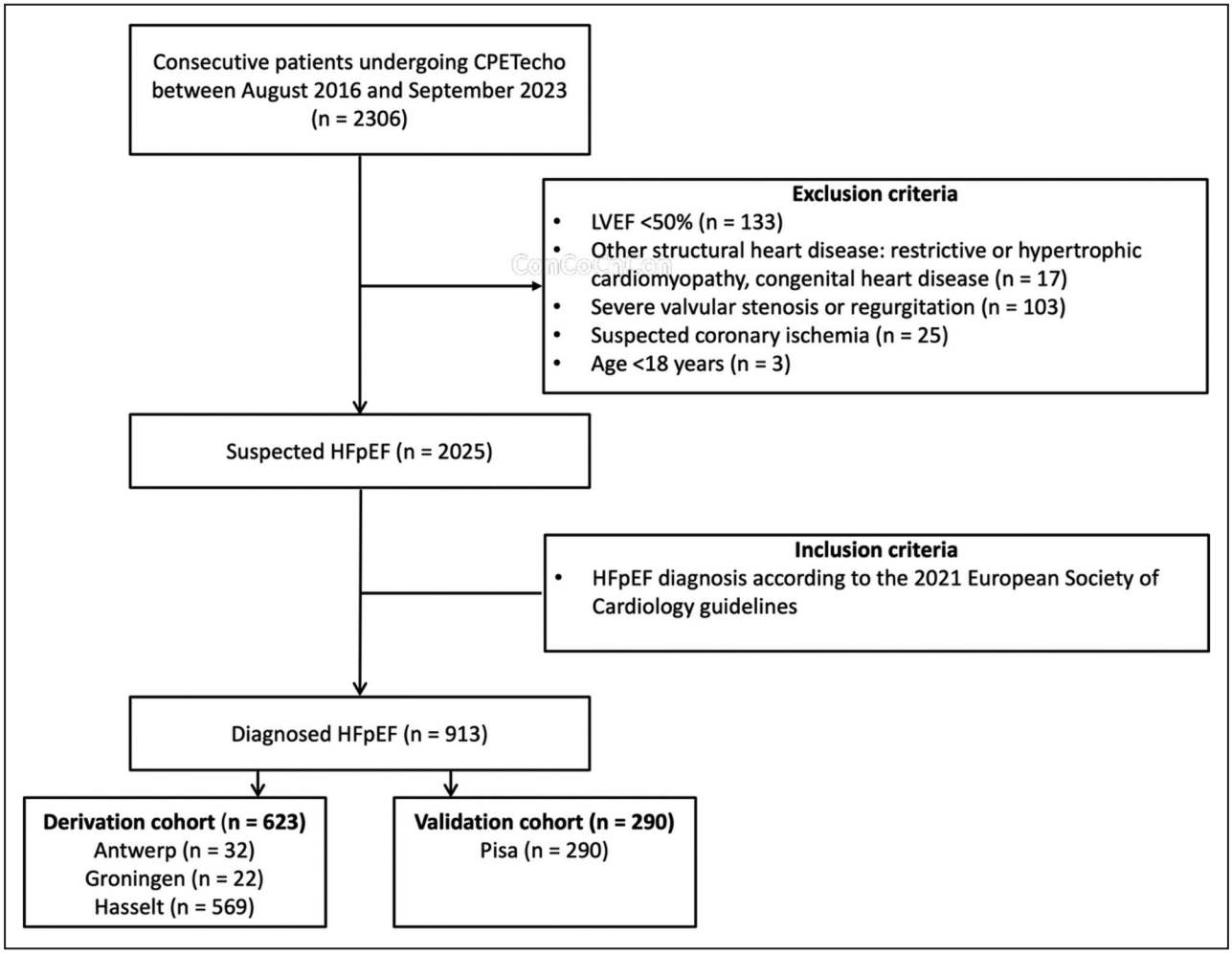

Figure 1. Patient selection flow chart.
Of all 2306 patients referred for CPETecho, 913 met eligibility criteria. CPETecho indicates combined cardiopulmonary exercise testing and exercise echocardiography; HFpEF, heart failure with preserved ejection fraction; and LVEF, left ventricular ejection fraction.

and highest cardiac output/VO_2 slope. Phenotype 3 (n=158, 25%) was characterized by reduced right ventricular (RV) reserve and lowest peak tricuspid annular plane systolic excursion/systolic PAP. Patients with phenotype 4 (n=107, 17%) exhibited impaired LV stroke volume reserve during exercise, paralleled by the highest body mass index. In contrast, phenotype 5 (n=134, 22%) showed the poorest exercise capacity, moderately reduced LV and RV systolic function, the lowest cardiac power output, most severe left atrial remodeling, and pronounced chronotropic incompetence with many on negative chronotropic medication. Moreover, these patients had the lowest estimated glomerular filtration rate, highest NT-proBNP levels, and were more likely to have a history of coronary artery disease, as well as to be treated with loop diuretics and mineralocorticoid receptor antagonists. As a sensitivity analysis, we included a pairwise comparison of the clusters (Table S3), and repeated clustering using the Leiden algorithm, which yielded very similar results to the initial analysis (Table S4, Figures S4 and S5). Additionally, we performed a sensitivity analysis including only patients with an H_2FPEF score ≥6. This yielded a much smaller population (n=197 patients in the derivation cohort, n=120 in the validation cohort) in which the exercise phenotypes 1 to 5 could not clearly be distinguished (Figure S6).

External Validation

The validation cohort successfully replicated all 5 clusters (Figure 4A) with a similar distribution of patients across phenotypes. Patient characteristics according to HFpEF exercise phenotypes in the validation cohort are presented in Table S5 and Figure S7. All CPETecho variables were consistently elevated or reduced across clusters in both derivation and validation cohorts (Figure 4B). The overall intraclass correlation coefficient

Table 1. Baseline Characteristics of the Total Study Population: Derivation Versus Validation Cohorts

	Derivation (n=623)	Validation (n=290)	*P* value
Demographic data			
Age, y	74 (69–79)	76 (71–82)	<0.001
Female sex, n (%)	378 (61)	137 (47)	<0.001
Height, cm	167 (159–172)	168 (159–174)	0.273
Weight, kg	75 (65–87)	75 (65–85)	0.653
Body mass index, $kg.m^{-2}$	27.3 (24.0–31.0)	26.7 (23.9–30.3)	0.346
Systolic blood pressure, mmHg	145±23	135±20	<0.001
Diastolic blood pressure, mmHg	78 (71–87)	75 (65–85)	0.001
Heart rate, bpm	68±12	77±13	<0.001
Rhythm, n (%)			
Sinus	558 (90)	216 (75)	<0.001
Atrial fibrillation	60 (10)	51 (18)	
Negative chronotropic medication, n (%)	440 (70)	199 (69)	0.687
History, n (%)			
Hypertension	435 (70)	234 (81)	0.001
Atrial fibrillation	258 (41)	114 (39)	0.596
Diabetes	116 (19)	70 (24)	0.066
Coronary artery disease	131 (21)	41 (14)	0.017
Cerebrovascular disease	12 (2)	20 (7)	<0.001
Peripheral arterial disease	18 (3)	16 (6)	0.078
Laboratory			
Hemoglobin, $g.dL^{-1}$	13.4 (12.4–14.3)	12.7 (11.8–13.9)	<0.001
N-terminal prohormone B-type natriuretic peptide, $ng.L^{-1}$	340 (190–660)	528 (244–1208)	<0.001
Creatinine, $mg.dL^{-1}$	1.01 (0.84–1.26)	0.96 (0.81–1.20)	0.020
Estimated glomerular filtration rate, $mL.min^{-1}.1.73m^2$	61 (48–73)	66 (54–81)	<0.001
Heart failure with preserved ejection fraction scores			
H_2FPEF score	4 (3–6)	5 (3–6)	<0.001
HFA-PEFF score rest	4 (3–5)	5 (4–6)	<0.001
HFA-PEFF score exercise	6 (5–7)	6 (5–8)	<0.001
Echocardiographic parameters at rest			
LV ejection fraction (%)	61±8	63±7	0.011
TAPSE, cm	1.7 (1.2–2.2)	2.0 (1.8–2.3)	<0.001
E/A	0.9 (0.8–1.2)	1.0 (0.8–1.4)	0.517
E/e'	14.4±6.2	17.3±8.3	<0.001
Tricuspid regurgitation gradient, mm Hg	25±7	39±13	<0.001
LAVi, $mL.m^{-2}$	33±14	43±12	<0.001
LV mass index, $g.m^{-2}$	93±27	119±29	<0.001

Mean±SD for continuous variables (compared using independent samples *t* test after assessment of normality and homogeneity of variance using the Brown–Forsythe test; when variances were unequal, Welch's *t* test was applied), median (interquartile range) for nonparametric distribution (compared using Mann–Whitney *U* test), *n* (%) for categorical variables (compared using chi-square). *P* value <0.05 is considered significant. H_2FPEF indicates Heavy, Hypertensive, atrial Fibrillation, Pulmonary hypertension, Elder, Filling pressure score; HFA-PEFF, Heart Failure Association Pretest Probability Echocardiography and natriuretic peptide score, Functional Testing, and Final aetiology algorithm; E/A, ratio of early (E) to late (A) mitral valve flow velocity; E/e', ratio of E over early diastolic septal annular velocity (e'); LAVi, left atrial volume index; LV, left ventricular; and TAPSE, tricuspid annular plane systolic excursion.

of the magnitude of change of CPETecho variables between derivation and validation cohorts was 0.946 (*P*<0.001), with individual clusters ranging from 0.759 to 0.974 (all *P*<0.001, Table S6). Bland–Altman analysis further supported these findings, showing a mean difference near zero and 94% of variables falling within the 95% limits of agreement (Figure S8). Together, these findings confirm that the patterns discovered in the derivation cohort are well preserved in the independent validation cohort.

Clinical Outcomes According to HFpEF Phenogroups

During a mean follow-up of 3.0±1.8 years, a total of 160 combined clinical end point events were recorded in

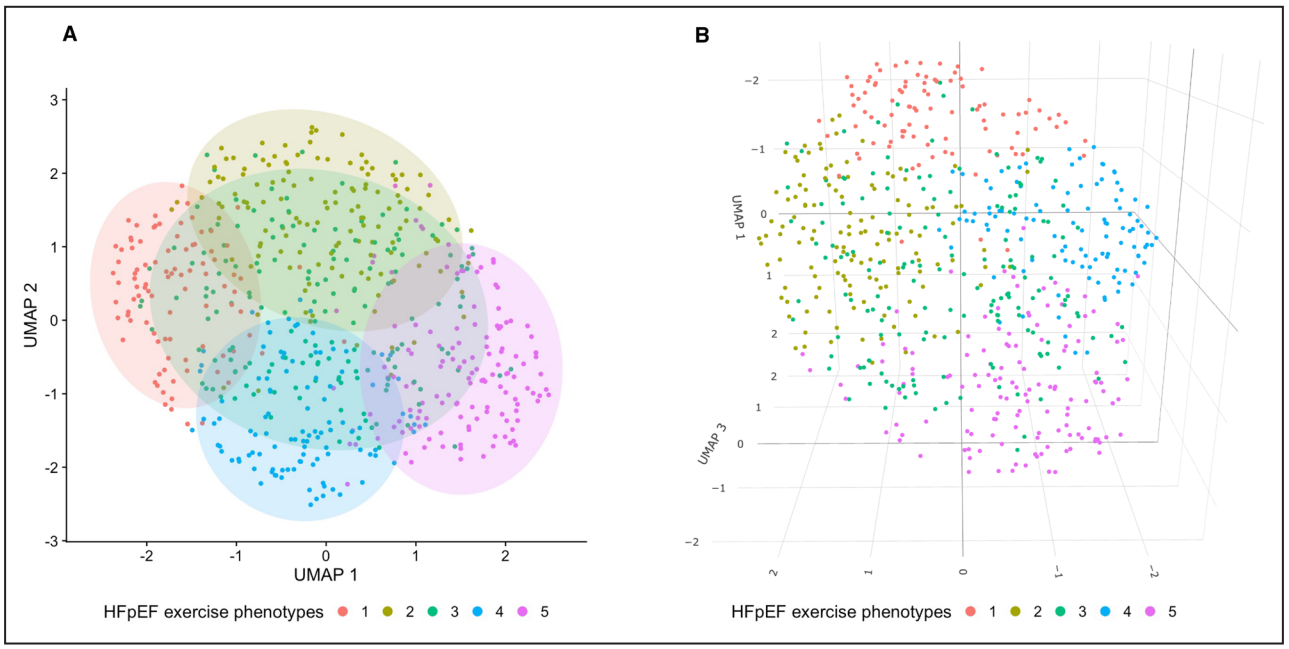

Figure 2. Visualization of HFpEF exercise phenotypes after dimensionality reduction in the derivation cohort.
A, Grouping of phenotypes projected onto a 2-dimensional space using UMAP, a technique used to simplify complex data by reducing it to 2 or 3 dimensions. This 2-dimensional embedding provides an initial visual grouping of the phenotypes, allowing observation of broad patterns between clusters. **B**, Grouping of phenotypes based on 3-dimensional UMAP embeddings. The additional dimension helps to reveal clearer separation and more explicit discrimination between the phenotypes, highlighting finer structural differences that may be less apparent in the 2-dimensional representation. See Video S1. HFpEF indicates heart failure with preserved ejection fraction; and UMAP, uniform manifold approximation and projection.

the derivation cohort, comprising 24 deaths and 136 unplanned cardiovascular hospitalizations (including 44 atrial fibrillation hospitalizations, 33 HF hospitalizations, and 14 acute coronary syndromes). Using phenotype 1 as a reference (12% with a primary outcome event), phenotype 5 showed significantly higher incidence of adverse events (37%), followed by 30% in phenotype 2 and 24% in phenotype 4 (Table 3). These associations remained significant after adjusting for age, sex, body mass index, hemoglobin, estimated glomerular filtration rate, NT-proBNP, and HFpEF risk scores (H_2FPEF and Heart Failure Association pretest probability echocardiography [HFA-PEFF] score; Table 3).

In the validation cohort (mean follow-up 2.0±1.3 years), 92 combined primary outcome events were recorded, with phenotype 3 showing a significantly higher incidence in unadjusted analysis. However, this association was no longer significant after multivariable adjustment (Table 3).

In the combined cohorts, Kaplan–Meier curves demonstrated significant differences in prognosis according to exercise phenotypes (log-rank P=0.003; Figure 5). In adjusted Cox regression analysis, phenotypes 2 (hazard ratio [HR], 1.76 [95% CI, 1.07–2.91]), 4 (HR, 2.15 [95% CI, 1.27–3.65]), and 5 (HR, 2.19 [95% CI, 1.33–3.61]) were each associated with worse outcomes compared with phenotype 1 (Table 3). The proportional hazards assumption was not violated. Kaplan–Meier curves for the derivation and validation cohorts individually are provided in Figures S9 and S10.

Exercise Phenotype Web Tool

To support clinical application, we developed a publicly accessible web tool (Figure S11) that enables phenotype classification in individual patients with HFpEF using a mutual nearest neighbors algorithm. This can be accessed at https://sdeschutter.shinyapps.io/Determining_HFpEF_exercise_phenotypes/.

DISCUSSION

In 913 patients with HFpEF who underwent advanced exercise testing with CPETecho, we identified 5 distinct HFpEF exercise phenotypes with significant differences in pathophysiological features, exercise capacity, and clinical outcomes. The response to acute exercise was remarkably heterogeneous, ranging from a phenotype with solitary lower diastolic reserve to an advanced phenotype with marked limitations in several cardiac and noncardiac domains. Several subgroups demonstrated specific exercise limitations, including impaired peripheral oxygen extraction, low LV systolic reserve, and RV-pulmonary artery uncoupling, highlighting the

Table 2. Baseline Characteristics of the Derivation Cohort, Stratified According to 5 HFpEF Exercise Phenotypes Identified in CPETecho-Based Cluster Analysis

Characteristics	Phenotype 1	Phenotype 2	Phenotype 3	Phenotype 4	Phenotype 5	*P* value
Total	93	131	158	107	134	
Demographic data						
Female sex, n (%)	38 (41)	73 (56)	115 (73)	68 (64)	84 (63)	<0.001
Age, y	70±8	74±8	74±7	72±7	75±9	<0.001
Body mass index, $kg.m^{-2}$	27.6±4.5	26.7±5.3	27.4±4.8	28.6±5.7	28.2±5.5	0.042
<25, n (%)	27 (29)	55 (42)	56 (35)	36 (34)	39 (29)	
25–30, n (%)	36 (39)	42 (32)	58 (37)	29 (27)	53 (40)	0.167
>30, n (%)	30 (32)	34 (26)	44 (28)	42 (39)	42 (31)	
Rhythm, n (%)						0.203
Sinus rhythm	85 (91)	124 (95)	139 (90)	93 (87)	117 (87)	
Atrial fibrillation	8 (9)	6 (5)	16 (10)	13 (12)	17 (13)	
History of, n (%)						
Hypertension	61 (66)	89 (68)	112 (71)	70 (65)	103 (77)	0.264
Atrial fibrillation	40 (43)	39 (30)	57 (36)	52 (49)	70 (52)	0.001
Diabetes	18 (19)	28 (21)	22 (14)	15 (14)	33 (25)	0.104
Coronary artery disease	14 (15)	27 (21)	34 (22)	16 (15)	40 (30)	0.030
Cerebrovascular disease	2 (2)	2 (2)	3 (2)	3 (3)	2 (2)	0.951
Peripheral arterial disease	1 (1)	2 (2)	8 (5)	2 (2)	5 (4)	0.253
Laboratory						
Hemoglobin, $g.dL^{-1}$	13.9 (12.8–15.0)	13.2 (12.3–14.15)	13.4 (12.4–14.17)	13.7 (12.8–14.3)	12.9 (12.3–13.8)	<0.001
N-terminal prohormone B-type natriuretic peptide, $ng.L^{-1}$	238 (130–372)	300 (170–480)	310 (200–680)	362 (193–650)	590 (340–980)	0.002
Creatinine, $mg.dL^{-1}$	1.04 (0.88–1.25)	0.97 (0.78–1.19)	0.98 (0.82–1.20)	1.08 (0.86–1.26)	1.14 (0.90–1.37)	<0.001
Estimated glomerular filtration rate, $mL.min^{-1}.1.73\ m^2$	67±20	64±23	63±20	60±15	53±21	<0.001
Therapy						
Negative chronotropic medication, n (%)	52 (57)	90 (69)	108 (70)	71 (68)	110 (83)	0.001
Angiotensin-converting enzyme inhibitor/ angiotensin receptor blocker, n (%)	10 (22)	24 (41)	51 (43)	19 (38)	32 (40)	0.183
Mineralocorticoid receptor antagonist, n (%)	3 (7)	11 (19)	30 (25)	4 (8)	25 (31)	0.002
Calcium channel blocker, n (%)	11 (24)	13 (22)	24 (20)	5 (10)	16 (20)	0.417
Statin, n (%)	19 (42)	25 (43)	58 (49)	19 (38)	35 (43)	0.753
Loop diuretics, n (%)	7 (16)	10 (17)	19 (16)	5 (10)	24 (30)	0.042
Thiazide, n (%)	4 (9)	11 (19)	32 (27)	9 (18)	10 (12)	0.036
Oral antidiabetic, n (%)	4 (9)	3 (5)	13 (11)	1 (2)	11 (14)	0.159
Insulin, n (%)	2 (4)	1 (2)	4 (3)	1 (2)	2 (3)	0.914
Sodium-glucose cotransporter 2 inhibitor, n (%)	0 (0)	0 (0)	1 (1)	0 (0)	0 (0)	0.741
Exercise capacity						
Peak respiratory exchange ratio	1.08 (1.05–1.12)	1.08 (1.03–1.14)	1.07 (1.01–1.15)	1.08 (1.02–1.12)	1.05 (1.00–1.12)	0.285
Peak workload, watt	98 (78–121)	74 (58–91)	58 (45–77)	75 (57–96)	48.5 (32.0–64.3)	<0.001
Peak VO_2, $mL.kg^{-1}.min$	17.1 (14.5–20.8)	14.5 (12.5–18.0)	12.6 (10.2–15.0)	14.6 (12.0–17.0)	10.8 (8.7–13.0)	<0.001
Peak VO_2, %predicted	89 (76–100)	82 (71–95)	76 (60–86)	83 (67–94)	64 (47–78)	<0.001
VE/VCO_2 slope	30±5	33±7	33±9	32±8	36±8	<0.001
Blood pressure response						
Systolic blood pressure, rest, mm Hg	148 (139–166)	141 (130–150)	151 (140–171)	137±22	138 (123–149)	<0.001
Diastolic blood pressure, rest, mm Hg	84 (77–92)	75 (69–83)	82 (74–91)	78 (71–88)	73 (64–82)	<0.001
Systolic blood pressure, peak, mm Hg	178±27	176±29	186±28	170±25	161±28	<0.001

(*Continued*)

Table 2. Continued

Characteristics	Phenotype 1	Phenotype 2	Phenotype 3	Phenotype 4	Phenotype 5	*P* value
Diastolic blood pressure, peak, mm Hg	88±17	76±14	84±16	82±13	71±14	0.001
CPOM, rest, watt/100 g	0.74 (0.56–0.90)	0.66 (0.53–0.87)	0.70 (0.52–0.92)	0.44 (0.35–0.60)	0.48 (0.38–0.65)	<0.001
CPOM, peak, watt/100 g	1.89 (1.46–2.21)	1.59 (1.14–2.04)	1.45 (1.20–1.74)	0.99 (0.77–1.31)	0.85 (0.62–1.08)	<0.001
Systolic blood pressure/workload slope	0.51 (0.38–0.72)	0.56 (0.35–0.81)	0.59 (0.32–1.00)	0.55 (0.36–0.90)	0.54 (0.31–1.01)	0.648
Arterial elastance, rest, mm Hg.mL^{-1}	1.9 (1.6–2.3)	1.5 (1.3–1.7)	2.1 (1.8–2.5)	2.2 (1.8–2.7)	2.0 (1.6–2.3)	<0.001
Arterial elastance, peak, mm Hg.mL^{-1}	2.2±0.5	1.7±0.4	2.2±0.6	2.3±0.5	2.1±0.6	<0.001
Total arterial compliance, rest, mL.mm Hg^{-1}	1.2±0.5	1.4±0.5	1.0±0.4	1.2±0.7	1.1±0.5	<0.001
Total arterial compliance, peak, mL.mm Hg^{-1}	0.7 (0.6–1.0)	1.0 (0.8–1.2)	0.7 (0.6–0.9)	0.8 (0.6–1.0)	0.8 (0.6–1.1)	<0.001
Heart rate response						
Heart rate, rest, bpm	71±12	65±11	71±13	68±13	65±11	<0.001
Heart rate, peak, bpm	129 (114–142)	112 (97–121)	113 (102–126)	113 (99–122)	89 (80–100)	<0.001
Heart rate reserve, %predicted	73 (58–91)	56 (41–73)	56 (44–74)	56 (44–64)	31 (22–42)	<0.001
VO_2/heart rate, rest, mL	3.7 (2.7–4.5)	3.6 (2.7–5.0)	3.1 (2.6–4.1)	3.5 (2.8–4.8)	3.8 (2.7–5.1)	0.008
VO_2/heart rate, peak, mL	10.5 (8.7–13.0)	10.3 (8.2–12.3)	8.0 (6.3–10.0)	10.1 (8.1–12.5)	8.9 (7.2–10.9)	<0.001
LV systolic function						
LVEF, rest, %	63±8	62±7	63±9	60±8	60±8	<0.001
LVEF, peak, %	68±12	66±9	68±11	65±10	63±10	0.008
SV, rest, mL	74.1±17.2	84.9±15.3	66.6±14	57.6±14.6	64.8±16.2	<0.001
SV, peak, mL	85.1 (75.5–98.4)	97.1 (86.9–108.4)	76.5 (68.0–86.6)	67.5 (57.5–76.8)	73.4 (62.3–85.4)	<0.001
SVi, rest, mL.m^{-2}	36.9 (32.5–42.2)	45.3 (41.1–51.0)	36.1 (31.7–41.1)	28.7 (25.2–34.0)	34.2 (29.0–40.0)	<0.001
SVi, peak, mL.m^{-2}	44.7 (40.6–48.4)	53.7 (48.1–58.7)	42.1 (37.4–47.3)	35.0 (30.8–40.4)	39.7 (33.8–46.5)	<0.001
CI, rest, L.min^{-2}.m^2	2.6 (2.3–3.0)	2.9 (2.5–3.4)	2.5 (2.2–2.9)	1.9 (1.7–2.3)	2.1 (1.9–2.5)	<0.001
CI, peak, L.min^{-2}.m^2	5.7 (5.0–6.6)	5.7 (5.1–6.5)	4.9 (4.3–5.4)	4.0 (3.4–4.6)	3.7 (3.1–4.1)	<0.001
Ventricular-arterial coupling, rest	0.52 (0.37–0.64)	0.43 (0.33–0.56)	0.48 (0.33–0.63)	0.64 (0.51–0.86)	0.56 (0.41–0.71)	<0.001
Ventricular-arterial coupling, peak	0.34 (0.26–0.46)	0.33 (0.26–0.40)	0.34 (0.23–0.48)	0.47 (0.34–0.59)	0.41 (0.29–0.53)	<0.001
LV diastolic function						
E, rest, m.s^{-1}	0.57 (0.47–0.64)	0.75 (0.62–0.90)	0.76 (0.62–0.88)	0.62 (0.54–0.78)	0.91 (0.75–1.11)	<0.001
A, rest, m. s^{-1}	0.69 (0.60–0.80)	0.81 (0.68–0.94)	0.79 (0.65–0.98)	0.66 (0.55–0.76)	0.67 (0.49–0.92)	<0.001
E, peak, m. s^{-1}	1.10±0.28	1.30±0.30	1.29±0.29	1.14±0.24	1.29±0.30	<0.001
E/A, rest	0.77 (0.65–0.91)	0.90 (0.78–1.11)	0.90 (0.71–1.14)	0.92 (0.78–1.20)	1.18 (0.91–2.14)	<0.001
E/e′, rest	10.5 (8.2–12.0)	13.1 (11.2–15.9)	14.4 (11.6–17.2)	11.6 (9.1–13.6)	17.2 (14.3–20.5)	<0.001
E/e′, highest	11.4 (9.1–14.0)	15.6 (13.6–17.3)	16.3 (14.1–18.7)	12.8 (10.5–15.5)	18.6 (15.7–23.7)	<0.001
Left heart morphology						
Left atrial volume index, mL.m^{-2}	32±13	36±14	29±11	32±15	37±15	<0.001
LV mass index, g.m^{-2}	90 (76–103)	92 (77–111)	88 (71–106)	90 (76–112)	90 (75–107)	0.421
Relative wall thickness	43 (36–49)	42 (36–50-	44 (37–51)	40 (33–45)	42 (37–48)	0.055
LVEDV index, rest, mL.m^{-2}	53.7±16.5	53.2±15.2	47.2±14.1	50.1±15.0	47.3±14.1	<0.001
LVEDV index, peak, mL.m^{-2}	54.3±16.5	55.0±13.9	46.6±13.4	50.7±14.3	47.6±13.9	<0.001
Right ventricle and pulmonary circulation						
TAPSE, rest, cm	2.0 (1.6–2.4)	2.2 (1.8–2.4)	1.2 (0.9–1.6)	1.8 (1.4–2.1)	1.6 (1.1–2.0)	<0.001
TAPSE, peak, cm	2.5 (2.0–2.9)	2.6 (2.3–2.8)	1.7 (1.3–2.0)	2.2 (1.9–2.5)	1.9 (1.4–2.3)	<0.001
RV S′, rest, cm. s^{-1}	10.0 (8.3–11.1)	10.8 (8.9–13.0)	7.0 (6.0–10.0)	8.3 (7.0–10.0)	7.0 (5.5–9.0)	<0.001
RV S′, peak, cm. s^{-1}	15.5±4.3	14.7±3.1	10.6±3.0	12.5±3.0	9.7±3.3	<0.001
TAPSE/PAPs, rest, mm.mm Hg^{-1}	0.89 (0.72–1.05)	0.89 (0.71–1.12)	0.46 (0.37–0.63)	0.74 (0.61–0.94)	0.56 (0.40–0.71)	<0.001
TAPSE/PAPs, peak, mm.mm Hg^{-1}	0.50 (0.39–0.61)	0.53 (0.45–0.61)	0.32 (0.25–0.41)	0.43 (0.39–0.49	0.37 (0.27–0.46)	<0.001
mPAP/CO slope, mmHg.L^{-1}.min^{-1}	2.8±1.2	3.0±1.5	4.1±1.8	4.7±2.1	6.4±4.2	<0.001
mPAP, peak, mm Hg	32±6	32±6	34±6	32±7	34±10	0.017

(*Continued*)

Table 2. Continued

Characteristics	Phenotype 1	Phenotype 2	Phenotype 3	Phenotype 4	Phenotype 5	*P* value
PAPs, rest, mm Hg	22 (19–26)	23 (21–28)	25 (22–30)	23 (19–26)	26 (23–32)	<0.001
PAPs, peak, mm Hg	49±9	49±9	53±10	50±10	53±16	0.019
HFpEF scores						
H_2FPEF score	4 (2–6)	3 (3–5)	4 (3–6)	5 (3–6)	5 (3–6)	<0.001
HFA-PEFF score, rest	5 (4–5)	4 (4–5)	4 (3–5)	5 (3–5)	5 (4–6)	0.227
HFA-PEFF score, exercise	5 (4–6)	6 (5–7)	6 (5–7)	5 (4–6)	7 (5–8)	<0.001
Pulmonary function						
FEV_1, %predicted	88 (74–97)	83 (69–96)	80 (63–91)	82 (72–93)	77 (59–88)	<0.001
FEV_1/FVC, %predicted	79±11	78±12	77±15	80±10	79±13	0.678
Oxygen saturation, rest, %	98±1	98±1	98±1	98±1	98±2	0.808
Oxygen saturation, peak, %	97±2	97±3	97±3	97±3	97±4	0.314
Breathing reserve, %	40 (30–48)	40 (30–52)	40 (28–49)	42 (32–51)	44 (29–54)	0.371
Peripheral						
CO/VO_2 slope	5.3±1.8	6.4±2.5	6.2±2.1	4.0±1.5	5.0±3.0	<0.001
AVO_2 difference, peak, mL/dL	12.2 (10.9–14.8)	10.4 (8.7–12.3)	10.7 (8.7–12.3)	14.9 (13.0–17.3)	12.4 (9.9–15.2)	<0.001
AVO_2 difference corrected for hemoglobin, peak, mL/g	0.90 (0.77–1.04)	0.80 (0.65–0.94)	0.81 (0.66–0.96)	1.12 (0.97–1.22)	0.95 (0.78–1.21)	<0.001

Mean±SD for continuous variables (compared using ANOVA after confirmation of normality of residuals and homogeneity of variance using the Brown–Forsythe test; when variances were unequal Welch's ANOVA was applied), median (interquartile range) for nonparametric distribution (compared using Kruskal–Wallis test), n (%) for categorical variables (compared using chi-square test). *P* value <0.05 is considered significant. AVO_2 indicates peripheral oxygen extraction; CI, cardiac index; CO, cardiac output; CPETecho, combined cardiopulmonary exercise testing and stress echocardiography; CPOM, cardiac power output-to-mass; E/A, ratio of early (E) to late (A) mitral valve flow velocity; E/e′, ratio of E over early diastolic septal annular velocity (e′); FEV_1, forced expiratory volume in 1 second; FVC, forced vital capacity; H_2FPEF, Heavy, Hypertensive, atrial Fibrillation, Pulmonary hypertension, Elder, Filling pressure score; HFA-PEFF, Heart Failure Association Pretest Probability, Echocardiography and natriuretic peptide score, Functional Testing, and Final aetiology algorithm; HFpEF, heart failure with preserved ejection fraction; LV, left ventricular; LVEDV, Left ventricular end-diastolic volume; LVEF, left ventricular ejection fraction; mPAP/CO slope, mean pulmonary artery pressure over cardiac output slope; PAPs, systolic pulmonary artery pressure; RV S′, peak systolic velocity of the lateral tricuspid annulus; SV, stroke volume; SVi, indexed stroke volume; TAPSE, tricuspid annular plane systolic excursion; VE/VCO_2, ventilation over carbon dioxide production slope; ventricular-arterial coupling, estimated as end-systolic volume/stroke volume;[45] and VO_2, oxygen uptake.

diverse mechanisms contributing to exercise intolerance in HFpEF.

Role of Exercise Testing in HFpEF Phenotyping

Phenotypical heterogeneity is a well-known feature of HFpEF and has been cited as one of the reasons so few large-scale clinical trials have met their primary end point.[6,10] Previous studies attempting to find subgroups in this heterogeneous population have largely relied on imaging at rest, biomarkers, and comorbidities.[6–8,10,24] This approach may overlook patients with dynamic abnormalities that become evident only during physical exertion.[5,13,25,26] Exercise intolerance in HFpEF is known to arise not only from diastolic dysfunction, but also from several other cardiac and extracardiac mechanisms.[27] Evaluating the cardiovascular, respiratory, and peripheral responses to exercise using CPETecho or invasive exercise testing offers a more comprehensive and physiologically meaningful characterization. Our analysis is the largest to date of this kind, applying unsupervised machine learning to a comprehensive set of CPETecho measurements. A previous study demonstrated the utility of CPETecho in phenotyping HFpEF based on 21 variables in 265 Asian patients, identifying 3 phenogroups.[28] Notably, their groups 1 and 2 correspond to our "phenotype 1" and "phenotype 3" classifications. A study using invasive hemodynamic testing in 397 patients with HFpEF in the United States found 3 phenogroups, including 2 groups corresponding to our "phenotype 1" and "phenotype 5."[6] Differences between our findings may reflect variations in HFpEF characteristics between populations, the broader set of CPETecho variables used in our analysis, and different methodology.

Pathophysiological Characteristics of HFpEF Exercise Phenotypes and Their Clinical Impact

The broader aim of phenotyping in HFpEF is to move beyond uniform treatment strategies and enable more personalized therapeutic approaches. We provide a framework for such personalized treatment based on our results. However, it remains unclear whether distinct phenotypes differ in their response to current

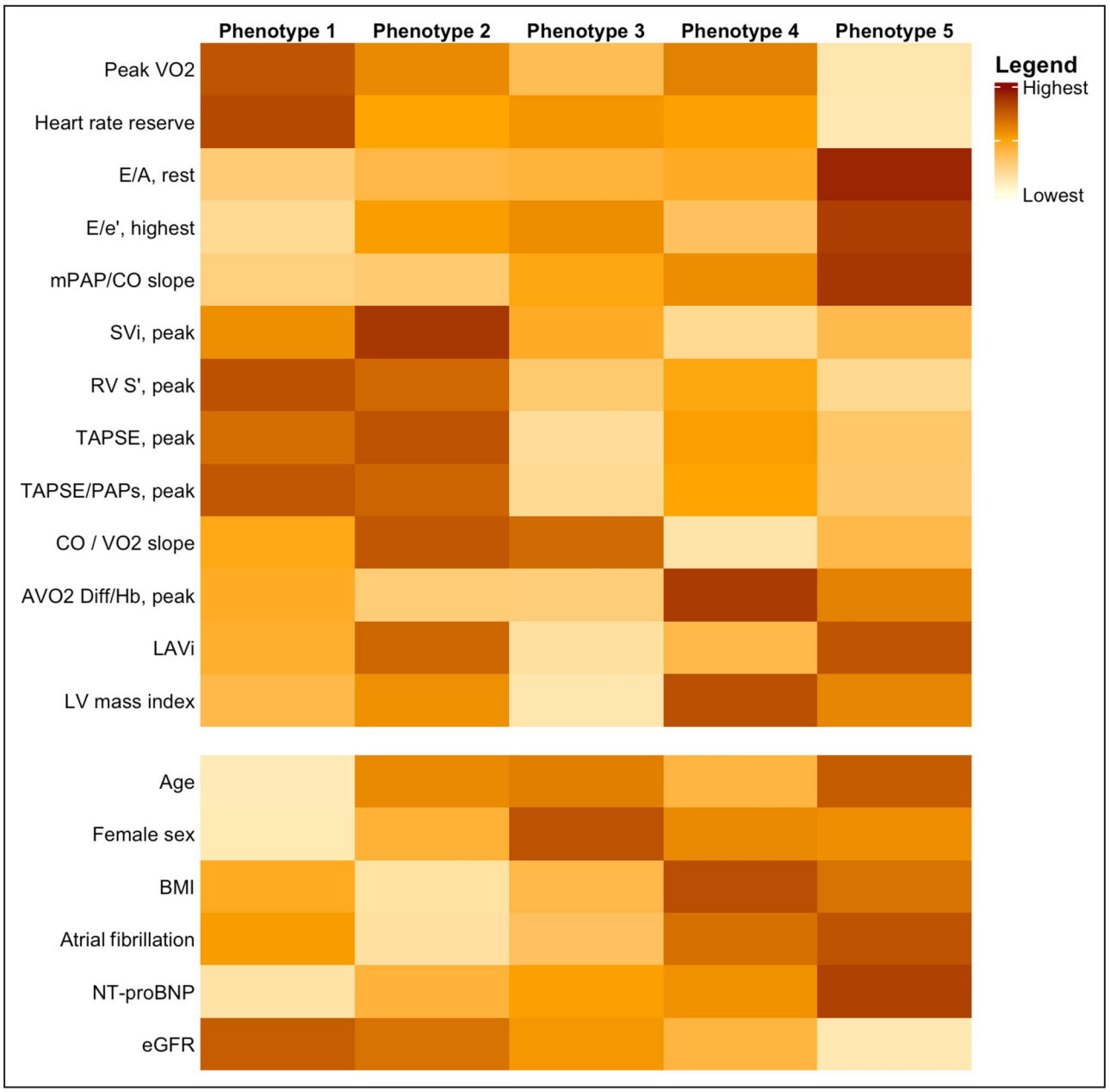

Figure 3. HFpEF phenotypes based on exercise limitations.
Heatmap of clinical and CPETecho characteristics (rows) according to HFpEF exercise phenotypes (columns). Darker rectangles indicate higher values of the respective characteristic. AVO_2 diff indicates peripheral oxygen extraction; BMI, body mass index; CO, cardiac output; E/A, ratio of early (E) to late (A) mitral valve flow velocity; E/e′, transmitral blood flow (E) over early diastolic septal mitral annular velocity (e′); eGFR, estimated glomerular filtration rate; Hb, hemoglobin; highest, highest value obtained from either submaximal or maximal exercise stages; LAVI, left atrial volume index; LV, left ventricular; mPAP/CO slope, mean pulmonary artery pressure over cardiac output slope; NT-proBNP, N-terminal prohormone B-type natriuretic peptide; PAPs, systolic pulmonary artery pressure; RV S′, peak systolic velocity of the lateral tricuspid annulus; SVi, indexed stroke volume; TAPSE, tricuspid annular plane systolic excursion; and VO_2, oxygen uptake.

treatments, highlighting the need for further investigation. Furthermore, assigning a single label to each phenotype disregards the considerable differences in exercise response, and multiple labels may apply to a given phenotype.

Phenotype 1: This low-risk phenotype is marked by mild diastolic dysfunction, minimal myocardial remodeling and preserved biventricular cardiac function, consistent with an "early HFpEF" stage.[6,28] Patients are slightly younger and have the lowest NT-proBNP

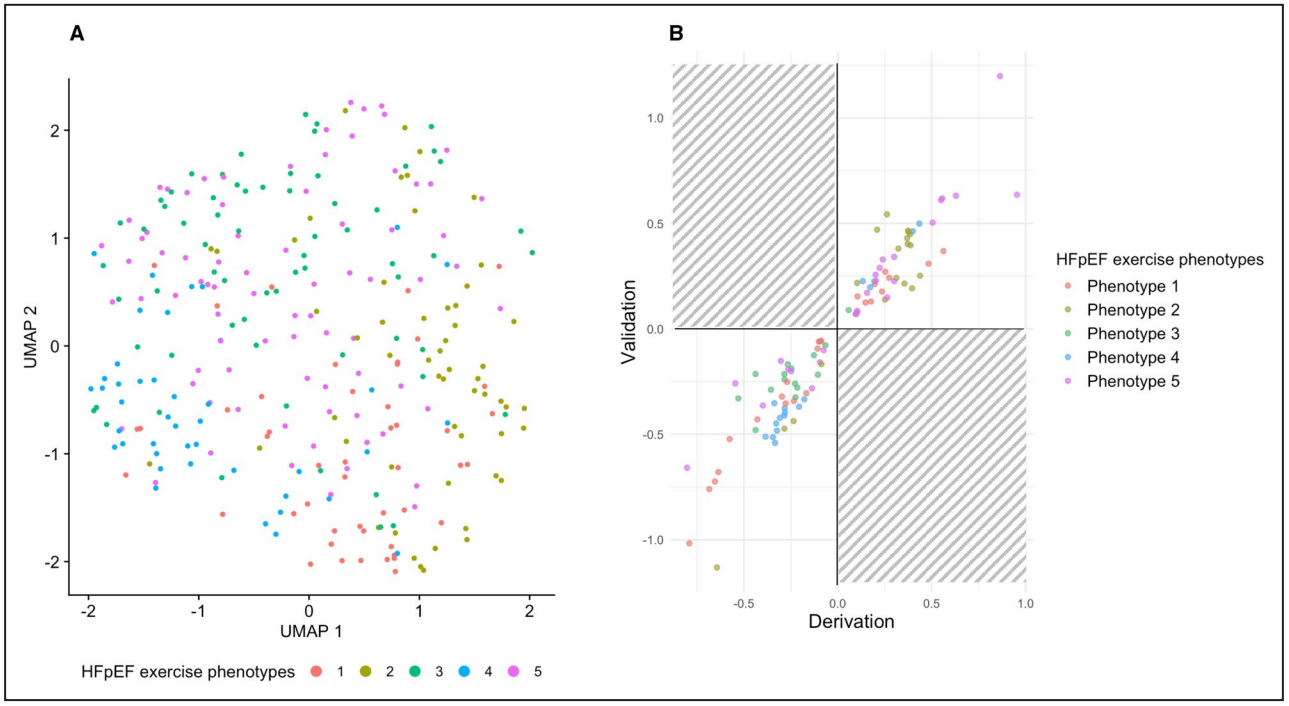

Figure 4. External validation of exercise phenotypes.
A, Grouping of phenotypes in validation cohort based on 2-dimensional UMAP embeddings. All clusters could be reproduced in the validation cohort. **B**, Consistency of variable expression in derivation and validation data sets. Each dot represents a variable that was identified as significantly associated with 1 of the 5 HFpEF exercise phenotypes used in the clustering analysis. The *x* axis shows the log2 fold change of the variable in the derivation cohort, indicating how strongly that variable is elevated or reduced in a specific phenotype compared with others. The *y* axis shows the log2 fold change of the same variable in the validation cohort. All variables demonstrate consistent elevation or reduction in each cluster in both data sets. Specifically, variables in the upper right quadrant are elevated in a given cluster in both data sets, whereas those in the lower left quadrant are reduced in a given cluster in both data sets. The absence of dots in the upper left and lower right shaded quadrants indicates that no variable shows opposing patterns between data sets. HFpEF indicates heart failure with preserved ejection fraction; and UMAP, uniform manifold approximation and projection.

levels, though 1 in 8 patients still experienced a primary outcome event over a mean follow-up of 3 years. Given the limited cardiac remodeling, this phenotype may represent a critical window for early intervention, with the potential to slow or even reverse disease progression. Early initiation of SGLT2i, combined with lifestyle changes such as structured physical activity and dietary interventions may help delay advancement. Subanalyses from the TOPCAT (Treatment of Preserved Cardiac Function Heart Failure With an Aldosterone Antagonist) and I-PRESERVE (Irbesartan in Heart Failure With Preserved Ejection Fraction) trials showed that patients with HFpEF with low H_2FPEF scores (≤6) and low NT-proBNP levels (<330 pg/mL) responded more favorably to spironolactone and irbesartan, respectively.[29,30] These findings highlight the importance of early intervention in HFpEF before irreversible pathological changes occur.

Phenotype 2: Impaired peripheral oxygen extraction has been proposed as a key contributor to exercise intolerance in HFpEF,[31] with skeletal muscle oxygenation being the primary determinant in the absence of anemia or lung disease.[32,33] Our findings identified a unique subgroup where reduced peripheral oxygen extraction seems the primary exercise-limiting factor. Exercise training improves quality of life and peak VO_2 in patients with HFpEF,[34,35] possibly through changes in skeletal muscle including enhanced mitochondrial efficiency and increased capillary density.[32,33] However, not all patients with HFpEF experience significant VO_2peak improvements with training. Efforts to identify predictors of response, such as baseline clinical, resting echocardiography, or isolate exercise echocardiography parameters, have not yet proven reliable.[36] It can be hypothesized that patients in this phenotype may show a superior response to exercise therapy, which could guide better selection for exercise-based programs in future trials. Moreover, these patients exhibited an increased risk of cardiovascular events despite relatively preserved LV and RV function, and lower levels of NT-proBNP. A recent study corroborates that reduced peripheral oxygen extraction recovery after exercise (<41%) is independently associated with increased mortality and heart failure hospitalization in patients with HFpEF or pulmonary

Table 3. Association of HFpEF Exercise Phenotypes With Adverse Outcomes Using Cox Proportional Hazards Analysis

Phenotypes	Events (% with primary outcome)	Unadjusted hazard ratio (95% CI)	*P* value	Adjusted hazard ratio* (95% CI)	*P* value
Derivation cohort					
Phenotype 1	11 (12)	Reference			
Phenotype 2	39 (30)	2.45 (1.26–4.79)	0.008	2.28 (1.13–4.57)	0.020
Phenotype 3	35 (22)	1.36 (0.69–2.68)	0.374	1.37 (0.67–2.83)	0.390
Phenotype 4	26 (24)	2.20 (1.08–4.44)	0.029	2.25 (1.10–4.62)	0.027
Phenotype 5	49 (37)	2.82 (1.47–5.43)	0.002	2.52 (1.24–5.14)	0.011
Validation cohort					
Phenotype 1	12 (25)	Reference			
Phenotype 2	16 (29)	1.31 (0.62–2.77)	0.478	1.08 (0.50–2.34)	0.840
Phenotype 3	25 (38)	2.64 (1.31–5.29)	0.006	1.91 (0.86–4.20)	0.110
Phenotype 4	14 (33)	2.13 (0.98–4.64)	0.057	2.08 (0.93–4.66)	0.074
Phenotype 5	25 (32)	1.88 (0.94–3.79)	0.074	1.29 (0.59–2.81)	0.517
Combined derivation and validation cohort					
Phenotype 1	23 (16)	Reference			
Phenotype 2	55 (29)	1.90 (1.17–3.09)	0.010	1.76 (1.07–2.91)	0.026
Phenotype 3	60 (27)	1.57 (0.97–2.55)	0.064	1.66 (0.99–2.77)	0.051
Phenotype 4	40 (27)	2.05 (1.23–3.43)	0.006	2.15 (1.27–3.65)	0.004
Phenotype 5	74 (35)	2.37 (1.49–3.79)	<0.001	2.19 (1.33–3.61)	0.002

*Adjusted for age, sex, body mass index, hemoglobin, estimated glomerular filtration rate, N-terminal prohormone B-type natriuretic peptide, Heavy, Hypertensive, Atrial Fibrillation, Pulmonary Hypertension, Elder, Filling Pressure (H_2FPEF) score and Heart Failure Association Pretest Probability Echocardiography, Functional Testing, Final Diagnosis (HFA-PEFF) score (rest and exercise). *P* value <0.05 is considered significant.

hypertension.[37] The prognostic significance of peripheral limitations in HFpEF remains incompletely understood and warrants further investigation in future studies.

Phenotype 3: Marked by the lowest tricuspid annular plane systolic excursion/systolic PAP ratios during exercise and impaired RV function, this group indicates an "HFpEF with RV-pulmonary artery uncoupling"

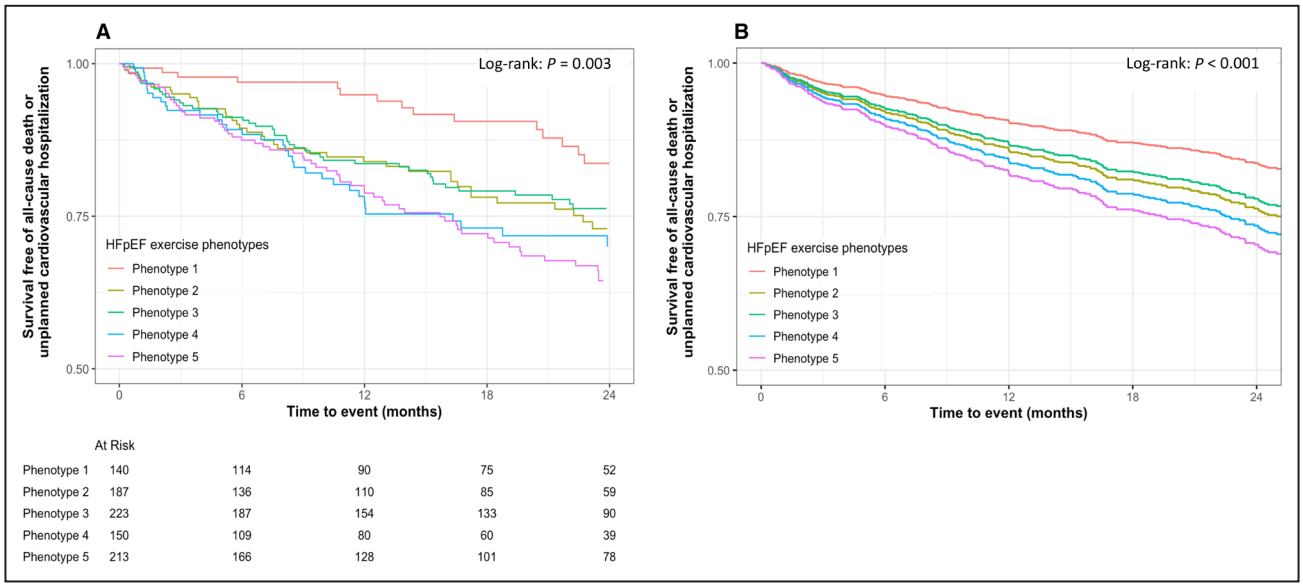

Figure 5. Survival free of all-cause death or unplanned cardiovascular hospitalization, stratified by HFpEF exercise phenotype.
A, Kaplan–Meier curves showing differences across HFpEF exercise phenotypes for the combined clinical end point of all-cause death and unplanned cardiovascular hospitalization in the combined derivation and validation cohort of 913 patients with HFpEF. **B**, Adjusted Cox survival curves showing differences across HFpEF exercise phenotypes for the combined clinical end point, accounting for age, sex, body mass index, hemoglobin, estimated glomerular filtration rate, N-terminal prohormone B-type natriuretic peptide, and HFpEF risk scores. HFpEF indicates heart failure with preserved ejection fraction.

phenotype. In HFpEF, pulmonary hypertension often begins as a passive consequence of elevated left atrial pressures associated with LV diastolic dysfunction and left atrial myopathy, leading to an increased pulsatile load on the right ventricle and RV dysfunction. Chronic pulmonary congestion can further trigger reactive increases in pulmonary arterial tone and pulmonary vascular remodeling, further worsening RV afterload and impairing LV preload.[38,39] This phenotype highlights the potential role of early pulmonary vascular changes in HFpEF pathophysiology. To date, drugs targeting RV afterload (ie, pulmonary hypertension) have not been proven beneficial in HFpEF.[39,40] However, recent evidence suggests SGLT2i may offer specific benefit in this context.[41]

Phenotype 4: This "HFpEF with low LV systolic reserve" group is associated with higher obesity rates. Visceral adiposity may contribute to HFpEF development through chronic inflammation, endothelial dysfunction, ventricular-vascular stiffness, and coronary microvascular dysfunction.[42,43] Epicardial adipose tissue may additionally lead to HF through lipid infiltration and pericardial constraint.[44] These mechanisms likely underlie the impaired stroke volume reserve observed in this group, also characterized by a high arterial elastance and reduced ventricular-arterial coupling.[45] Treatment with renin–angiotensin–aldosterone system inhibitors has been associated with improved stroke volume in HFpEF, though this did not translate into an increased exercise capacity or improved clinical outcomes.[31] Therapeutic strategies targeting obesity-driven mechanisms may be especially suited for this phenotype. Semaglutide improved HF-related symptoms, NT-proBNP levels, exercise capacity, and weight loss in patients with obesity and HFpEF.[46] Similarly, tirzepatide reduced cardiovascular events and improved health status.[47] Both traditional weight loss strategies, SGLT2i, and these novel metabolic agents effectively reduce epicardial adipose tissue.[44] Future studies in this phenotype could benefit from including myocardial strain metrics such as global longitudinal strain and LV work index to refine assessment of contractile reserve and uncover patients with HFpEF with subclinical systolic dysfunction.[14]

Phenotype 5: This phenotype represented a high-risk subgroup and can be addressed as "HFpEF with advanced functional impairment," characterized by the poorest exercise capacity, marked chronotropic incompetence, and signs of both LV and RV systolic dysfunction. Additionally, they exhibited the worst kidney function and, importantly, the poorest clinical outcomes with over one third experiencing a primary event at mean follow-up of 3 years. Chronotropic incompetence—linked with autonomic dysfunction, sinus node remodeling and β-receptor desensitization—is common in HFpEF and progressively worsens across advancing HFpEF stage.[48] In this advanced phenotype, chronotropic incompetence was likely influenced by widespread use of negative chronotropic agents (83% of patients). We can speculate that this subgroup may particularly benefit from β-blocker withdrawal, which has shown short-term benefits in patients with HFpEF and chronotropic incompetence; however, long-term impact remains unclear.[49] Additionally, cardiac pacing is being investigated as a treatment option not only for patients with concomitant conduction abnormalities but for all patients with HFpEF.[50] For patients with HFpEF at high risk of HF hospitalization, advanced therapies such as implantable hemodynamic monitors should be considered as part of long-term management.[15]

A phenogroup approach to classifying patients with HFpEF has several advantages over direct interpretation of individual physiological variables. Because patients with HFpEF often exhibit multiple, coexisting exercise limitations, it is not always straightforward to determine which impairment is most pathophysiologically relevant or therapeutically targetable in a given case. Clustering similar patients may uncover reproducible phenotypic patterns that reflect dominant physiological themes within each phenogroup and may become particularly helpful when clinical limitations overlap. For example, although chronotropic incompetence may occur across multiple phenotypes, its clinical management would likely differ if present in phenotype 2 (HFpEF with peripheral impairment) versus phenotype 5 (HFpEF with advanced functional impairment), for example, targeting peripheral conditioning and reconditioning in general versus heart rate modulation.

To support practical application, we developed a publicly available web tool enabling clinicians to classify patients with HFpEF into 1 of the 5 phenotypes using CPETecho data. This tool enhances clinical utility by allowing rapid and reproducible assignment of patients to data-driven phenotypes at the point of care, facilitating individualized diagnosis, prognostication, and enabling future phenotype-specific management strategies.

LIMITATIONS

An inherent shortcoming of unsupervised clustering is the requirement to categorize patients into distinct groups rather than acknowledging phenotypic overlap.[51] Moreover, phenotypes may evolve. This underscores the need for prospective, longitudinal research to understand the dynamic evolution. Medication use varied across phenotypes, and its potential influence on our findings cannot be ruled out. However, the clusters showed multiple linked physiologic impairments, reflecting broader pathophysiology rather than

isolated treatment effects. Notably, the use of SGLT2i was low in our cohort with HFpEF, as many patients were enrolled before the therapy was approved for HFpEF. Although future studies should explore how SGLT2i affect these distinct HFpEF phenotypes, they are unlikely to eliminate the underlying pathophysiological heterogeneity. Although phenotypes were reproducible in an external cohort, baseline characteristic differences suggest potential regional or institutional influences. Future studies should explore the applicability of these phenotypes in populations with varying ethnicities, care settings and comorbidity profiles including a broader body mass index spectrum, such as Asian or American cohorts. Outcomes did not significantly differ in the validation cohort after multivariable adjustment, likely due to shorter follow-up and lower number of events in this cohort. In the pooled analysis of both cohorts, prognostic differences across phenotypes remained statistically significant in both unadjusted and multivariable-adjusted Cox models. Further research is needed to determine whether classification by exercise phenotypes improves outcomes compared with "standard" HFpEF diagnosis. In a sensitivity analysis limited to patients with an H_2FPEF score ≥6, the 5 exercise phenotypes could no longer be clearly distinguished—likely due to the significantly reduced sample size. We did not include myocardial strain imaging, which may have enhanced sensitivity for detecting subtle systolic impairment.[14] Although CPETecho offers a comprehensive, noninvasive evaluation of exercise hemodynamics it has limitations: while pulmonary and RV parameters have demonstrated excellent correlation with exercise magnetic resonance imaging,[52] peripheral oxygen extraction difference remains an indirect estimate and may need confirmation using invasive catheterization or alternative techniques. Additionally, direct estimation of pulmonary artery wedge pressure is not possible, and transmitral blood flow over septal mitral annular peak velocity has its known limitations. Finally, supine exercise bicycles have weight limits (135–150 kg in this study), thus individuals with severe obesity may be underrepresented.

CONCLUSIONS

This study underscores the heterogeneity of HFpEF and the value of exercise-based phenotyping. Using CPETecho and unsupervised machine learning, we identified 5 distinct HFpEF exercise phenotypes, each characterized by unique responses to exercise, aerobic capacity, and prognosis. This phenotypic classification offers a foundation for more personalized, targeted treatment strategies in HFpEF, addressing an unmet need in this complex syndrome.

ARTICLE INFORMATION

Received March 20, 2026; accepted June 10, 2026.

Affiliations

Research group Cardiovascular Diseases, GENCOR Department, University of Antwerp, Antwerp, Belgium (S.D.S., C.M.V.d., A.B.G.); Department of Cardiology, Antwerp University Hospital (UZA), Edegem, Belgium (S.D.S., C.M.V.d., A.B.G.); Department of Clinical and Experimental Medicine, University of Pisa, Pisa, Italy (N.R.P., N.D.B., L.D.P., S.M.); University Medical Centre Groningen, Groningen, The Netherlands (L.M.M.); Department of Cardiology and Jessa & Science, Jessa Hospital, Hasselt, Belgium (S.M., J.S., L.H., G.C., J.V.); and UHasselt, Faculty of Medicine and Life Sciences/LCRC, Diepenbeek, Belgium (S.M., J.S., L.H., G.C., J.V.).

Sources of Funding

This project was carried out with the support of University of Antwerp (BOF DOCPRO 51265) to Andreas B. Gevaert, Research Foundation Flanders (FWO SB G041024N) to Stephanie De Schutter, and the Belgian Heart Foundation (Dumont prize 2024) to Andreas B. Gevaert managed by the King Baudouin Foundation.

Disclosures

Andreas B. Gevaert reports receiving research grants to his institution by Abbott and Boehringer Ingelheim and travel/lecture fees to his institution by Abbott, AstraZeneca, Boehringer Ingelheim, Johnson and Johnson, Menarini, Novartis, and Novo Nordisk; all outside the submitted work. Stephanie De Schutter reports receiving a research grant from AstraZeneca outside the submitted work. Laura M. G. Meems reports consulting/speaker horonaria received through her institution from AstraZeneca, Boehringer Ingelheim, Bayer, Bristol-Myers Squibb, Daiichi-Sankyo, Eli Lilly, Novartis, Novo Nordisk, Pfizer, Relaxera, and Vasa Therapeutics outside the submitted work. Caroline M. Van de Heyning reported receiving personal fees from Abbott, Bayer, Daiichi-Sankyo, Edwards Lifesciences, Menarini, and Pfizer outside the submitted work. Jan Verwerft received travel grants from AstraZeneca, Daiichi Sankyo Belgium, Novartis Pharma, Pfizer, Novo Nordisk Pharma, and St Jude Medical Belgium and speaker fees from AstraZeneca, Bayer, Novartis Pharma, Janssen-Cilag, and Daiichy Sankyo Belgium all unrelated to this work. Stefano Masi reports receiving personal fees from Servier.

Supplemental Material

Supplemental Methods
Tables S1–S6
Figures S1–S11
Video S1

REFERENCES

1. Lam CS, Donal E, Kraigher-Krainer E, Vasan RS. Epidemiology and clinical course of heart failure with preserved ejection fraction. *Eur J Heart Fail*. 2011;13:18–28. doi: 10.1093/eurjhf/hfq121
2. Shah KS, Xu H, Matsouaka RA, Bhatt DL, Heidenreich PA, Hernandez AF, Devore AD, Yancy CW, Fonarow GC. Heart failure with preserved, borderline, and reduced ejection fraction: 5-year outcomes. *J Am Coll Cardiol*. 2017;70:2476–2486. doi: 10.1016/j.jacc.2017.08.074
3. McDonagh TA, Metra M, Adamo M, Gardner RS, Baumbach A, Böhm M, Burri H, Butler J, Čelutkienė J, Chioncel O, et al. 2023 focused update of the 2021 ESC guidelines for the diagnosis and treatment of acute and chronic heart failure. *Eur Heart J*. 2023;44:3627–3639. doi: 10.1093/eurheartj/ehad195
4. Kondo T, Henderson AD, Docherty KF, Jhund PS, Vaduganathan M, Solomon SD, McMurray JJV. Why have we not been able to demonstrate reduced mortality in patients with HFmrEF/HFpEF? *J Am Coll Cardiol*. 2024;84:2233–2240. doi: 10.1016/j.jacc.2024.08.033
5. Gevaert AB, Kataria R, Zannad F, Sauer AJ, Damman K, Sharma K, Shah SJ, Van Spall HGC. Heart failure with preserved ejection fraction: recent concepts in diagnosis, mechanisms and management. *Heart*. 2022;108:1342–1350. doi: 10.1136/heartjnl-2021-319605
6. Shah SJ, Katz DH, Selvaraj S, Burke MA, Yancy CW, Gheorghiade M, Bonow RO, Huang CC, Deo RC. Phenomapping for novel classification of heart failure with preserved ejection fraction. *Circulation*. 2015;131:269–279. doi: 10.1161/circulationaha.114.010637

7. Woolley RJ, Ceelen D, Ouwerkerk W, Tromp J, Figarska SM, Anker SD, Dickstein K, Filippatos G, Zannad F, Metra M, et al. Machine learning based on biomarker profiles identifies distinct subgroups of heart failure with preserved ejection fraction. *Eur J Heart Fail*. 2021;23:983–991. doi: 10.1002/ejhf.2144
8. Gevaert AB, Tibebu S, Mamas MA, Ravindra NG, Lee SF, Ahmad T, Ko DT, Januzzi JL Jr, Van Spall HGC. Clinical phenogroups are more effective than left ventricular ejection fraction categories in stratifying heart failure outcomes. *ESC Heart Fail*. 2021;8:2741–2754. doi: 10.1002/ehf2.13344
9. Gevaert AB, Mueller S, Winzer EB, Duvinage A, Van de Heyning CM, Pieske-Kraigher E, Beckers PJ, Edelmann F, Wisløff U, Pieske B, et al. Iron deficiency impacts diastolic function, aerobic exercise capacity, and patient phenotyping in heart failure with preserved ejection fraction: a subanalysis of the OptimEx-Clin study. *Front Physiol*. 2021;12:757268. doi: 10.3389/fphys.2021.757268
10. Fraser AG, Tschöpe C, de Boer RA. Diagnostic recommendations and phenotyping for heart failure with preserved ejection fraction: knowing more and understanding less? *Eur J Heart Fail*. 2021;23:964–972. doi: 10.1002/ejhf.2205
11. Verwerft J, Bertrand PB, Claessen G, Herbots L, Verbrugge FH. Cardiopulmonary exercise testing with simultaneous echocardiography: blueprints of a dyspnea clinic for suspected HFpEF. *JACC Heart Fail*. 2023;11:243–249. doi: 10.1016/j.jchf.2022.11.004
12. Del Punta L, De Biase N, Armenia S, Di Fiore V, Maremmani D, Gargani L, Mazzola M, De Carlo M, Mengozzi A, Lomonaco T, et al. Combining cardiopulmonary exercise testing with echocardiography: a multiparametric approach to the cardiovascular and cardiopulmonary systems. *Eur Heart J Imaging Methods Pract*. 2023;1:qyad021. doi: 10.1093/ehjimp/qyad021
13. Pugliese NR, De Biase N, Gargani L, Mazzola M, Conte L, Fabiani I, Natali A, Dini FL, Frumento P, Rosada J, et al. Predicting the transition to and progression of heart failure with preserved ejection fraction: a weighted risk score using bio-humoural, cardiopulmonary, and echocardiographic stress testing. *Eur J Prev Cardiol*. 2021;28:1650–1661. doi: 10.1093/eurjpc/zwaa129
14. Smiseth OA, Donal E, Boe E, Ha JW, Fernandes JF, Lamata P. Phenotyping heart failure by echocardiography: imaging of ventricular function and haemodynamics at rest and exercise. *Eur Heart J Cardiovasc Imaging*. 2023;24:1329–1342. doi: 10.1093/ehjci/jead196
15. McDonagh TA, Metra M, Adamo M, Gardner RS, Baumbach A, Bo¨hm M, Burri H, Butler J, Celutkiene J, Chioncel O, et al. 2021 ESC guidelines for the diagnosis and treatment of acute and chronic heart failure. Developed by the task force for the diagnosis and treatment of acute and chronic heart failure of the European Society of Cardiology (ESC). *Eur Heart J*. 2021;42:3599–3726.
16. Pugliese NR, Fabiani I, Santini C, Rovai I, Pedrinelli R, Natali A, Dini FL. Value of combined cardiopulmonary and echocardiography stress test to characterize the haemodynamic and metabolic responses of patients with heart failure and mid-range ejection fraction. *Eur Heart J Cardiovasc Imaging*. 2019;20:828–836. doi: 10.1093/ehjci/jez014
17. Lancellotti P, Pellikka PA, Budts W, Chaudhry FA, Donal E, Dulgheru R, Edvardsen T, Garbi M, Ha JW, Kane GC, et al. The clinical use of stress echocardiography in non-Ischaemic heart disease: recommendations from the European Association of Cardiovascular Imaging and the American Society of Echocardiography. *J Am Soc Echocardiogr*. 2017;30:101–138. doi: 10.1016/j.echo.2016.10.016
18. Scali MC, Zagatina A, Simova I, Zhuravskaya N, Ciampi Q, Paterni M, Marzilli M, Carpeggiani C, Picano E. B-lines with lung ultrasound: the optimal scan technique at rest and during stress. *Ultrasound Med Biol*. 2017;43:2558–2566. doi: 10.1016/j.ultrasmedbio.2017.07.007
19. Wasserman K, Hansen JE, Sue DY, Whipp BJ. *Principles of Exercise Testing and Interpretation*. 1st ed. Philadelphia PA: Lea & Febiger; 1987.
20. Zappia L, Oshlack A. Clustering trees: a visualization for evaluating clusterings at multiple resolutions. *Gigascience*. 2018;7:7. doi: 10.1093/gigascience/giy083
21. Tibshirani R, Walther G, Hastie T. Estimating the number of clusters in a data set via the gap statistic. *J Royal Statis Soc Series B: Statis Method*. 2001;63:411–423. doi: 10.1111/1467-9868.00293
22. Charrad M, Ghazzali N, Boiteau V, Niknafs A. NbClust: an R package for determining the relevant number of clusters in a data set. *J Stat Softw*. 2014;61:1–36.
23. Stuart T, Butler A, Hoffman P, Hafemeister C, Papalexi E, Mauck WM 3rd, Hao Y, Stoeckius M, Smibert P, Satija R. Comprehensive integration of single-cell data. *Cell*. 2019;177:1888–1902.e1821. doi: 10.1016/j.cell.2019.05.031
24. Anker SD, Usman MS, Anker MS, Butler J, Böhm M, Abraham WT, Adamo M, Chopra VK, Cicoira M, Cosentino F, et al. Patient phenotype profiling in heart failure with preserved ejection fraction to guide therapeutic decision making. A scientific statement of the Heart Failure Association, the European Heart Rhythm Association of the European Society of Cardiology, and the European Society of Hypertension. *Eur J Heart Fail*. 2023;25:936–955. doi: 10.1002/ejhf.2894
25. Pugliese NR, Balletti A, Armenia S, De Biase N, Faita F, Mengozzi A, Paneni F, Ruschitzka F, Virdis A, Ghiadoni L, et al. Ventricular-arterial coupling derived from proximal aortic stiffness and aerobic capacity across the heart failure spectrum. *JACC Cardiovasc Imaging*. 2022;15:1545–1559. doi: 10.1016/j.jcmg.2022.03.024
26. Pugliese NR, De Biase N, Conte L, Gargani L, Mazzola M, Fabiani I, Natali A, Dini FL, Frumento P, Rosada J, et al. Cardiac reserve and exercise capacity: insights from combined cardiopulmonary and exercise echocardiography stress testing. *J Am Soc Echocardiogr*. 2021;34:38–50. doi: 10.1016/j.echo.2020.08.015
27. Pecchia B, Samuel R, Shah V, Newman E, Gibson GT. Mechanisms of exercise intolerance in heart failure with preserved ejection fraction (HFpEF). *Heart Fail Rev*. 2025;30:777–789. doi: 10.1007/s10741-025-10504-3
28. Saito Y, Omae Y, Harada T, Sorimachi H, Yuasa N, Kagami K, Murakami F, Naito A, Tani Y, Kato T, et al. Exercise stress echocardiography-based phenotyping of heart failure with preserved ejection fraction. *J Am Soc Echocardiogr*. 2024;37:759–768. doi: 10.1016/j.echo.2024.05.003
29. Segar MW, Patel KV, Berry JD, Grodin JL, Pandey A. Generalizability and implications of the H(2)FPEF score in a cohort of patients with heart failure with preserved ejection fraction. *Circulation*. 2019;139:1851–1853. doi: 10.1161/circulationaha.118.039051
30. Anand IS, Rector TS, Cleland JG, Kuskowski M, McKelvie RS, Persson H, McMurray JJ, Zile MR, Komajda M, Massie BM, et al. Prognostic value of baseline plasma amino-terminal pro-brain natriuretic peptide and its interactions with irbesartan treatment effects in patients with heart failure and preserved ejection fraction: findings from the I-PRESERVE trial. *Circ Heart Fail*. 2011;4:569–577. doi: 10.1161/circheartfailure.111.962654
31. Wolsk E, Kaye D, Komtebedde J, Shah SJ, Borlaug BA, Burkhoff D, Kitzman DW, Lam CSP, van Veldhuisen DJ, Ponikowski P, et al. Central and peripheral determinants of exercise capacity in heart failure patients with preserved ejection fraction. *JACC Heart Fail*. 2019;7:321–332. doi: 10.1016/j.jchf.2019.01.006
32. Gevaert AB, Böhm B, Hartmann H, Goovaerts I, Stoop T, Van De Heyning CM, Beckers PJ, Baldassarri F, Mueller S, Oberhoffer R, et al. Effect of training on vascular function and repair in heart failure with preserved ejection fraction. *JACC Heart Fail*. 2023;11:454–464. doi: 10.1016/j.jchf.2022.12.011
33. Winzer EB, Augstein A, Schauer A, Mueller S, Fischer-Schaepmann T, Goto K, Hommel J, van Craenenbroeck EM, Wisløff U, Pieske B, et al. Impact of different training modalities on molecular alterations in skeletal muscle of patients with heart failure with preserved ejection fraction: a substudy of the OptimEx trial. *Circ Heart Fail*. 2022;15:e009124. doi: 10.1161/circheartfailure.121.009124
34. Mueller S, Winzer EB, Duvinage A, Gevaert AB, Edelmann F, Haller B, Pieske-Kraigher E, Beckers P, Bobenko A, Hommel J, et al. Effect of high-intensity interval training, moderate continuous training, or guideline-based physical activity advice on peak oxygen consumption in patients with heart failure with preserved ejection fraction: a randomized clinical trial. *JAMA*. 2021;325:542–551. doi: 10.1001/jama.2020.26812
35. Edelmann F, Wachter R, Duvinage A, Mueller S, Fegers-Wustrow I, Schwarz S, Christle JW, Pieske-Kraigher E, Seyfarth M, Knapp M, et al. Combined endurance and resistance exercise training in heart failure with preserved ejection fraction: a randomized controlled trial. *Nat Med*. 2025;31:306–314. doi: 10.1038/s41591-024-03342-7
36. Gevaert AB, Winzer EB, Mueller S, De Schutter S, Beckers PJ, Hommel J, Linke A, Wisløff U, Adams V, Pieske B, et al. Training-induced change of diastolic function in heart failure with preserved ejection fraction. *ESC Heart Fail*. 2025;12:1652–1662. doi: 10.1002/ehf2.15225
37. El Shaer A, Garcia-Arango M, Abed A, Heffernan S, Wang Y, Javed T, Esmaeeli A, Arif AW, Tao R, Dharmavaram N, et al. Breaking down the recovery of O(2) pathway: peripheral extraction recovery pattern defines exercise capacity and clinical outcomes. *Physiol Rep*. 2025;13:e70337. doi: 10.14814/phy2.70337

38. Borlaug BA, Sharma K, Shah SJ, Ho JE. Heart failure with preserved ejection fraction: JACC scientific statement. *J Am Coll Cardiol*. 2023;81:1810–1834. doi: 10.1016/j.jacc.2023.01.049
39. Guazzi M, Naeije R. Right heart phenotype in heart failure with preserved ejection fraction. *Circ Heart Fail*. 2021;14:e007840. doi: 10.1161/circheartfailure.120.007840
40. Hoeper MM, Oerke B, Wissmüller M, Leuchte H, Opitz C, Halank M, Seyfarth HJ, Baldus S, Bauersachs J, Böhm M, et al. Tadalafil for treatment of combined postcapillary and precapillary pulmonary hypertension in patients with heart failure and preserved ejection fraction: a randomized controlled phase 3 study. *Circulation*. 2024;150:600–610. doi: 10.1161/circulationaha.124.069340
41. Reddy YNV, Carter RE, Sorimachi H, Omar M, Popovic D, Alogna A, Jensen MD, Borlaug BA. Dapagliflozin and right ventricular-pulmonary vascular interaction in heart failure with preserved ejection fraction: a secondary analysis of a randomized clinical trial. *JAMA Cardiol*. 2024;9:843–851. doi: 10.1001/jamacardio.2024.1914
42. Stoicescu L, Crişan D, Morgovan C, Avram L, Ghibu S. Heart failure with preserved ejection fraction: the pathophysiological mechanisms behind the clinical phenotypes and the therapeutic approach. *Int J Mol Sci*. 2024;25:25. doi: 10.3390/ijms25020794
43. Pugliese NR, Paneni F, Mazzola M, De Biase N, Del Punta L, Gargani L, Mengozzi A, Virdis A, Nesti L, Taddei S, et al. Impact of epicardial adipose tissue on cardiovascular haemodynamics, metabolic profile, and prognosis in heart failure. *Eur J Heart Fail*. 2021;23:1858–1871. doi: 10.1002/ejhf.2337
44. Dronkers J, van Veldhuisen DJ, van der Meer P, Meems LMG. Heart failure and obesity: unraveling molecular mechanisms of excess adipose tissue. *J Am Coll Cardiol*. 2024;84:1666–1677. doi: 10.1016/j.jacc.2024.07.016
45. Holm H, Magnusson M, Jujić A, Bozec E, Girerd N. How to calculate ventricular-arterial coupling? *Eur J Heart Fail*. 2022;24:600–602. doi: 10.1002/ejhf.2456
46. Kosiborod MN, Abildstrøm SZ, Borlaug BA, Butler J, Rasmussen S, Davies M, Hovingh GK, Kitzman DW, Lindegaard ML, Møller DV, et al. Semaglutide in patients with heart failure with preserved ejection fraction and obesity. *N Engl J Med*. 2023;389:1069–1084. doi: 10.1056/NEJMoa2306963
47. Packer M, Zile MR, Kramer CM, Baum SJ, Litwin SE, Menon V, Ge J, Weerakkody GJ, Ou Y, Bunck MC, et al. Tirzepatide for heart failure with preserved ejection fraction and obesity. *N Engl J Med*. 2025;392:427–437. doi: 10.1056/NEJMoa2410027
48. Zweerink A, van der Lingen ACJ, Handoko ML, van Rossum AC, Allaart CP. Chronotropic incompetence in chronic heart failure. *Circ Heart Fail*. 2018;11:e004969. doi: 10.1161/circheartfailure.118.004969
49. Palau P, Seller J, Domínguez E, Sastre C, Ramón JM, de La Espriella R, Santas E, Miñana G, Bodí V, Sanchis J, et al. Effect of β-blocker withdrawal on functional capacity in heart failure and preserved ejection fraction. *J Am Coll Cardiol*. 2021;78:2042–2056. doi: 10.1016/j.jacc.2021.08.073
50. Habel N, Infeld M, Bernknopf J, Meyer M, Lustgarten D. Rationale and design of the PACE HFpEF trial: physiologic accelerated pacing as a holistic treatment of heart failure with preserved ejection fraction. *Heart Rhythm O2*. 2024;5:41–49. doi: 10.1016/j.hroo.2023.12.001
51. Larson K, Omar M, Sorimachi H, Omote K, Alogna A, Popovic D, Tada A, Doi S, Naser J, Reddy YNV, et al. Clinical phenogroup diversity and multiplicity: impact on mechanisms of exercise intolerance in heart failure with preserved ejection fraction. *Eur J Heart Fail*. 2024;26:564–577. doi: 10.1002/ejhf.3105
52. Claessen G, La Gerche A, Voigt JU, Dymarkowski S, Schnell F, Petit T, Willems R, Claus P, Delcroix M, Heidbuchel H. Accuracy of echocardiography to evaluate pulmonary vascular and RV function during exercise. *JACC Cardiovasc Imaging*. 2016;9:532–543. doi: 10.1016/j.jcmg.2015.06.018